Electronic and magnetic structure of bcc nickel

N. B. Brookes,* A. Clarke,† and P. D. Johnson
Physics Department, Brookhaven National Laboratory, Upton, New York 11973
(Received 11 September 1991; revised manuscript received 15 January 1992)

The electronic and magnetic structure of metastable bcc nickel grown on Fe(001) has been investigated using spin-polarized angle-resolved photoemission. At the iron lattice constant bcc nickel is found to be ferromagnetic, with a moment of $(0.4\pm0.45)\mu_B$ in reasonable agreement with theoretical predictions, and with a Curie temperature above 300 K. A "6-eV" spin-polarized satellite is also observed, analogous to that seen for fcc nickel previously. The observation of spin polarization in this feature confirms the presence of long-range ferromagnetic order at the local nickel sites.

INTRODUCTION

The interest in magnetic materials has been spurred by the ability to realize metastable phases experimentally through epitaxial growth on single-crystal substrates acting as templates.[1] Examples include body-centered-cubic (bcc) cobalt,[2] face-centered-cubic (fcc) iron,[3] and bcc nickel.[4–6] Phase diagrams derived from total-energy calculations[7] for these bulk metastable structures predict a stable magnetic state at some lattice constant. In the ultrathin-film region [one to two monolayers (ML)], interesting properties, such an enhanced moments, have also been predicted.[8] These theoretical findings are mostly untested.

Recently, the structure of the bcc phase of nickel grown epitaxially on Fe(001) substrates has been studied using low-energy electron-diffraction[4] (LEED) and reflection high-energy electron-diffraction[5] (RHEED) techniques. For films less than about six layers, the nickel is found to grow in a bcc manner, and above this thickness a slight distortion occurs, eventually leading to $c(2\times2)$-like LEED and RHEED patterns. However, the structure seems to be more complicated than a simple $c(2\times2)$ reconstruction. The films are bcc-like, but the strained overlayer is thought to be relaxing by forming misfit dislocations.[6] LEED analysis[4] of bcc nickel showed that the structure mimics that of iron with very similar interlayer separations, including the small relaxations seen in iron.

Calculations[7] for the bcc phase of nickel show that the calculated equilibrium lattice spacing (2.773 Å) a nonmagnetic state is favored. However, a magnetic phase transition is expected to occur for a 1.5% expansion. Hence, at the iron-lattice spacing 2.866 Å (a 3.35% expansion), bcc nickel should be ferromagnetic.[7] The predicted moment is approximately $0.5\mu_B$, which is similar to that of fcc nickel. In addition, calculations[9] for ferromagnetic one- and two-layer nickel films on Fe(001) show that there are strong hybridization effects at the interface, leading to an interfacial iron moment which is enhanced slightly with respect to the bulk, but lower than the iron-surface atom moment.

Based on ferromagnetic resonance (FMR) line shifts, Heinrich *et al.*[5] suggested that bcc nickel grown on Fe(001) was ferromagnetic with a transition temperature above 80 K and that modeling of the FMR results was consistent with a $\sim0.4\mu_B$ nickel moment. Results at room temperature were inconclusive. More recently, polarized neutron-reflection (PNR) studies[10] of a 3-ML bcc nickel sample grown on five layers of iron have been undertaken. At 4 K, a nickel moment of $(0.55-0.80)\mu_B$ and an iron moment close to the bulk value $[(2.2-2.4)\mu_B]$ were found.

In the present spin-polarized photoemission study, we show that "bulklike" bcc nickel films grown on Fe(001) are ferromagnetic at room temperature with bands exchange split by approximately 0.3 eV. The spectra, however, are strongly influenced by correlation effects, which, in particular, give rise to satellite structure. There also appear to be interfacial or finite thickness effects in the thinner films.

EXPERIMENTAL DETAILS

The experiments reported here were carried out on an apparatus which is described in detail elsewhere.[11] Briefly, spin detection is achieved with a compact low-energy spin detector[12] and uses light provided by the U5 vacuum ultraviolet (vuv) undulator at the National Synchrotron Light Source. The angular resolution of the hemispherical analyzer was $\pm1.5°$, and the combined photon and analyzer energy resolution was 0.35 eV. The Fe(001) crystal was manufactured in the form of a picture frame with each leg along a ⟨100⟩ direction and magnetized using a coil wound around one leg. The crystal was cleaned by repeated argon-ion bombardment and annealing cycles. The surface contamination level was monitored initially using Auger-electron spectroscopy (AES) and in the final stages using photoelectron spectroscopy.

The epitaxial growth of the nickel overlayers was achieved using a liquid-nitrogen-cooled electron-beam bombardment source. The films were evaporated at room temperature, and the thickness was monitored using AES and calibrated against the work of Wang *et al.*[4] The structural quality of the films was monitored using LEED; the (1×1) overlayer patterns were of comparable quality to those of the substrate, which gave very sharp spots.

RESULTS

Figure 1 shows the normal-emission spin-polarized spectra from clean Fe(001) and a thick ($\sim$7 ML) bcc nickel film grown on the same substrate. For Fe(001) there is an overall bandwidth of about 2.5 eV, and the exchange splitting in the iron d bands is easily observed. In contrast, the bcc nickel d-band width is much narrower ($\sim$1 eV). However, the observation of exchange-split bands suggests that the bcc nickel film is probably ferromagnetic.

The peaks in the photoemission spectra of Fe(001), at $h\nu=60$ eV [Fig. 1(b)], correspond to transitions close to the $\Gamma_{25'}$ ($\Gamma_{25'}^{\uparrow}\approx 2.6$ eV, $\Gamma_{25'}^{\downarrow}\approx 0.3$ eV) and Γ_{12} ($\Gamma_{12}^{\uparrow}\approx 0.7$ eV) critical points,[13] the minority Γ_{12} critical point being above the Fermi level. The $\Gamma_{25'}$ and Γ_{12} critical points can be distinguished since they are of different symmetry and hence have opposite dependences on the polarization of the incident light. The peaks in the $h\nu=60$ eV photoemission spectrum from bcc nickel (at the iron-lattice constant) will also correspond to transitions close to the Γ critical point.

If nonorthogonal tight-binding parameters for fcc nickel[14] are scaled[15] and used to model bcc nickel, then the $\Gamma_{25'}$ critical points are found at higher binding energies than the Γ_{12} and all four are below the Fermi level. Consequently, the minority feature closest to the Fermi level is of Γ_{12} character in bcc nickel, where, as for iron, it is $\Gamma_{25'}$. If the nickel was in its fcc phase, then at 60 eV photon energy the transitions would occur from bands away from Γ, $\frac{1}{3}$ of the Γ to X direction.[16] By examining the band structure,[16,17] one finds (even when correlation effects are included[17]) that the two minority bands would occur above the two majority bands. Hence fcc and bcc nickel can be distinguished by knowing the positions of the minority and majority bands and their symmetries.

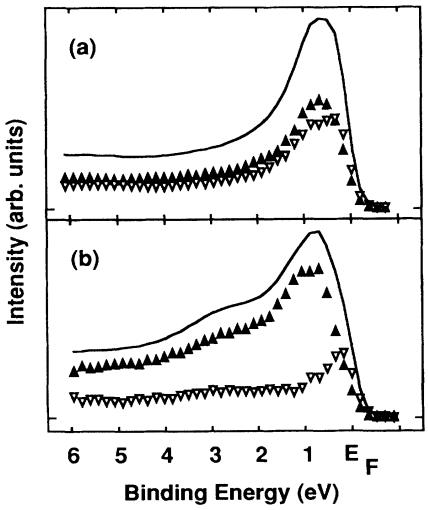

FIG. 1. Angle- and spin-resolved photoemission spectra taken at normal emission, $h\nu=60$ eV and 70° angle of incidence, for (a) bcc nickel [grown on Fe(001)] and (b) bcc iron [Fe(001)]. The spin-integrated spectra are shown as solid lines, and the majority and minority spectra are shown as up (▲) and down (▽) triangles, respectively.

The light-polarization dependence of the nickel peaks are shown in Fig. 2. It can be readily seen that the ordering of the minority (0.4 and 0.9 eV) and majority (0.7 and 0.9 eV) peaks is inconsistent with the fcc nickel phase. Also, the minority feature at 0.4 eV has the expected sensitivity for a Γ_{12}-derived peak (i.e., enhanced at p polarization), as does the majority feature at 0.7 eV binding energy; this is consistent with a bcc nickel phase. This gives an exchange splitting for the Γ_{12} critical point of 0.3 eV. The $\Gamma_{25'}$ exchange splitting is not resolvable (<0.1 eV), however. This may be due to the influence of additional features from the interface region or may be because the peaks are broad.

The Γ_{12} ($\Gamma_{25'}$) exchange splitting and bandwidth expected from a tight-binding model are approximately 0.5 eV (0.5 eV) and 2 eV, respectively, which compares with the experimental values of $\sim$0.3 eV (<0.1 eV) and $\sim$0.6 eV. Similar deviations from expected values have also been observed for fcc nickel and are correlated with the presence of a satellite approximately 6 eV below the valence band.

The origin of the nickel satellite has been the subject of considerable debate for many years.[18,19] It is now generally accepted to result from correlation effects, as is the narrowing of the d bands and the reduced exchange splitting. This excited-state phenomenon is atomic in origin and consequently is expected to occur independent of the structure.

At a photon energy of approximately 68 eV, the satellite is found to resonate.[19] Figure 3 shows the spectra for

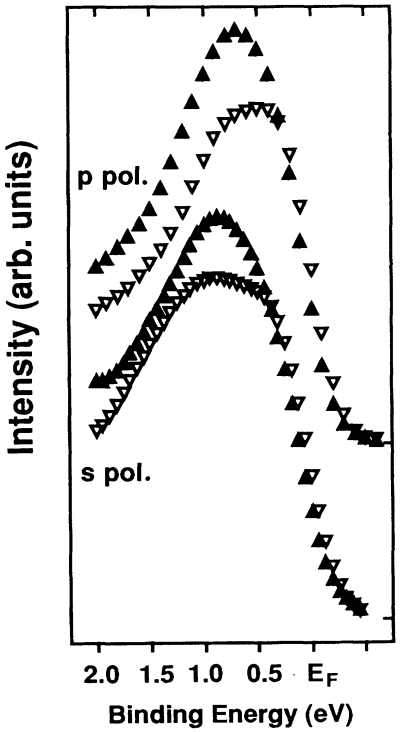

FIG. 2. Light polarization dependence of the spin-polarized valence-band structure for bcc nickel. The photon energy is $h\nu=60$ eV, and s- and p-polarized light refers to angles of the light of $\vartheta_i=35°$ and 70°, respectively.

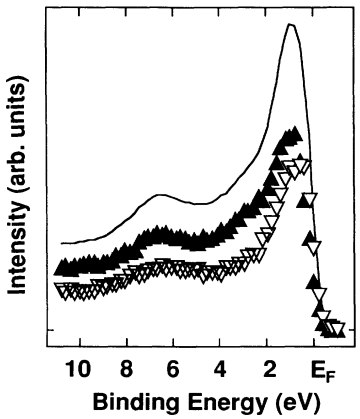

FIG. 3. Spin-polarized normal-emission photoemission spectra for bcc nickel. The photon energy is $h\nu=68$ eV and the angle of incidence $\vartheta_i=70°$. The spin-integrated spectrum is shown as a solid line, and the majority and minority spectra are shown as up (▲) and down (▽) triangles, respectively.

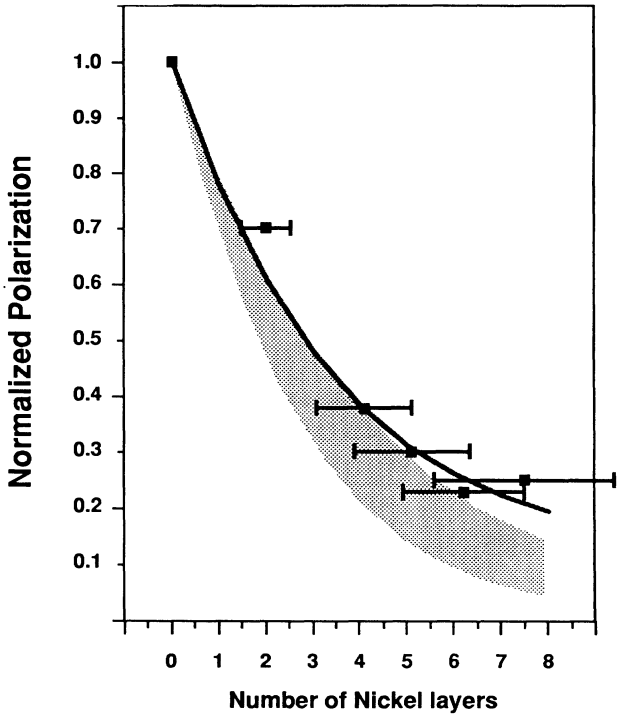

FIG. 4. Normalized polarization, $P(x)/P_s$ [see Eq. (1)], as a function of overlayer thickness for bcc nickel grown on Fe(001). The squares represent the experimental points. The horizontal error bars are shown, and the vertical error bars are less than the symbols. The shaded region gives the expected results assuming a nonmagnetic overlayer with a range of mean free paths (λ), $\lambda=4.5\pm1$ Å, and the solid line gives the result assuming a small nickel moment; see the text for details.

bcc nickel on resonance; a satellite is clearly observed. As for fcc nickel,[18] the summed intensity of the off-resonance satellite and Auger peak is less than the satellite intensity on resonance. The satellite was observed, independent of film thickness (4–8 ML), at a binding energy of 6.3± 0.1 eV. This binding energy is the same as is found for fcc nickel. One of the experiments which helped to establish the origin of the 6-eV satellite in fcc nickel was the confirmation of its predicted spin polarization.[20] We find that the satellite observed in the present study is also polarized, ~25%±9%. This observation is significant because the satellite is independent of band-structure effects and demonstrates that there is *long-range ferromagnetic order in bcc nickel at room temperature.*

Based on the above discussion, we believe that bcc nickel is ferromagnetic at room temperature. However, it is of obvious interest to know the magnitude of the nickel magnetic moment. In principle, an estimate of the moment can be obtained by considering the background polarization in the photoemission spectra. Figure 4 shows this background polarization (normalized to that of the substrate) for a series of film thicknesses. The error bars were determined from the uncertainties in the sample-thickness calibration and the statistical errors in determining the background polarization. Assuming layer-by-layer growth, it can be shown that the polarization as a function of coverage, $P(x)$ is given by

$$P(x)=\frac{P_s e^{-x/\lambda}+P_o R(1-e^{-x/\lambda})}{e^{-x/\lambda}+R(1-e^{-x/\lambda})}\ , \tag{1}$$

where P_s and P_o are the polarizations due to bulk samples of the substrate and overlayer, respectively. R is the ratio of the overlayer to substrate background emission, and λ is the spin-averaged mean free path of the photoemitted electrons. (For the electron energies under consideration here, i.e., ~50 eV, it has been shown[21] that there is no spin dependence in the mean free path.) The thickness x is given by $x=md$, where d is the interlayer thickness and m is the number of overlayers. For a nonmagnetic nickel overlayer (i.e., $P_o=0$), with values for the mean free path varying from $\lambda=3.5$ to 5.5 Å [$\lambda=4.5$ Å (Ref. 22) ±1.0 Å], $R=0.9$ (determined from the photoemission spectra), and x equated assuming an interlayer spacing of 1.433 Å,[4] evaluation of $P(x)/P_s$ leads to the shaded region in Fig. 4. This region, although intercepting the error bars of the data, is below the experimental values, suggesting a contribution to the polarization from the overlayer, i.e., ferromagnetic nickel. An estimate of the overlayer moment can be gained if we assume that the background polarization P is proportional to the local moment per atom, n_B, normalized to the number of valence electrons, n_V, thus

$$P\propto\frac{n_B}{n_V}\ . \tag{2}$$

If the proportionality constant is the same for the overlayer and substrate, a reasonable assumption in this case since the structures are very similar,[4] then given the moment per atom for bulk iron ($2.2\mu_B$) an estimate of the nickel moment can be made. (Our estimate might be expected to be slightly low, since the interfacial moment is calculated to be lower than that of the iron-surface atom.[9]) Reasonable agreement with the experiment is achieved, as is shown by the solid line in fig. 4, using for

nickel $n_V=9$, $R=0.9$, and $\lambda=4.5$ Å. This line gives us a moment per atom for bcc nickel of $(0.4\pm0.45)\mu_B$, (including the uncertainties in the various parameters), which is close to the calculated value for bcc nickel,[7] in agreement with the FMR models[5,6] and PNR results.[10] The Curie temperature is also well above room temperature since measurements at 300 and 150 K give essentially identical results for both the exchange splittings and background polarization.

Figure 5 shows the development of the bcc nickel structure from the ultrathin-film regime to the bcc nickel films considered above. In the clean iron minority spectra, there is a single peak at the Fermi level.[13] As the nickel layers develop, another minority feature can be seen at ~1 eV binding energy, and this becomes weaker as the thick-film regime is approached (Fig. 5). Similar changes are also occurring in the majority bands, but it is more difficult to see because of the larger bandwidth of the iron majority states.

In the ultrathin regime it is difficult, because of the strong iron d-band intensity, to identify exchange-split peaks, however, by ~4 ML the additional features can be distinguished by using the light polarization, and effects similar to those shown in Fig. 2 are seen for the thick film.

Thin-film calculations[9] indicate a strong hybridization of the iron and nickel d bands at the interface. However, because of the small exchange splittings involved and the similar iron and nickel cross sections, we have difficulty in separating the various contributions. As noted above, however, a distinct change occurs in the intermediate-thickness range, and this may reflect the transition from interfacial to more bulklike properties. Until the thick-film region is reached, it is difficult to determine whether or not additional spectral structure is clearly due to exchange-split peaks.

The result of the modeling shown in Fig. 4 shows that for 4–8 ML a nickel moment of $0.4\mu_B$ is not unreasonable and further suggests that, although we have difficulty interpreting the photoemission spectra, these films are ferromagnetic at room temperature. The result for the 2-ML nickel film is also intriguing since the point in Fig. 4 lies just above the model lines and might be interpretable in terms of enhanced interfacial moments. However, the accuracy of our measurements needs to be improved before this result can be definitive.

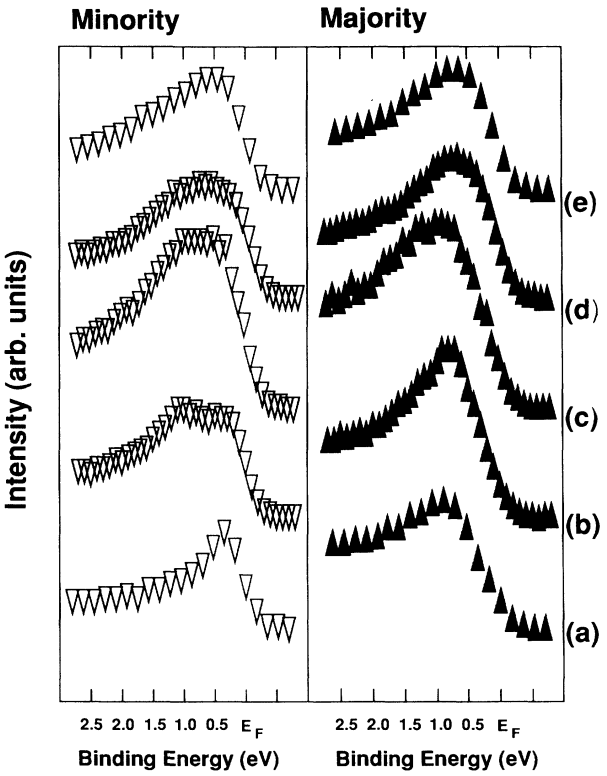

FIG. 5. Spin-resolved photoemission spectra taken at normal emission, $\vartheta_i=35°$ and $h\nu=60$ eV, for nickel overlayers grown on Fe(001). The majority and minority spectra are shown as up (▲) and down (▽) triangles, respectively, and correspond to the following coverages: (a) ~2.0 ML, (b) ~4.1 ML, (c) ~5.1 ML, (d) ~6.2 ML, and (e) ~7.5 ML.

SUMMARY

In summary, we have determined that bcc nickel at the iron-lattice spacing is indeed ferromagnetic, in agreement with the work of Moruzzi *et al.*[7] The Curie temperature is well above room temperature, and the results are consistent with the predicted moment of $0.5\mu_B$. Both the observed bandwidth and exchange splitting are reduced from the expected values, which, together with the presence of a 6-eV satellite and its spin polarization, demonstrate that correlation effects strongly affect the spectra, as is seen for fcc nickel. This in turn reconfirms the atomic origin of the satellite. Nickel films of 4–8 ML thickness appear to have similar moments $[(0.4\pm0.45)\mu_B]$, but the photoemission spectra for the thinner films show additional structure, which is possibly due to the interface.

ACKNOWLEDGMENTS

This work was supported in part by U.S. Department of Energy Contract No. DE-AC02-76CH00016 and National Science Foundation Materials Research Group Contract No. DMR-86-03304.

*Present address: ESRF, BP220, F-38043, Grenoble, CEDEX, France.

†Present address: Kodak Ltd., Surface Science W93, Healstone Drive, Harrow, Middlesex, HA1 40Y, UK.

[1] *Magnetism in Ultrathin Films,* edited by D. Pescia [special issue of Appl. Phys. A **49**, (1989)].

[2] G. A. Prinz, Phys. Rev. Lett. **54**, 1051 (1985).

[3] C. Liu, E. R. Moog, and S. D. Bader, Phys. Rev. Lett. **60**, 2422 (1988).

[4] P. M. Marcus, V. L. Moruzzi, Z. Q. Wang, Y. S. Li, and F.

Jona, in *Physical and Chemical Properties of Thin Metal Overlays and Alloy Surfaces,* edited by D. M. Zehner and D. W. Goodman, MRS Symp. Proc. No. 83 (Materials Research Society, Pittsburgh, 1986), p. 21; Z. Q. Wang, Y. S. Li, F. Jona, and P. M. Marcus, Solid State Commun. **61**, 623 (1987).

[5]B. Heinrich, A. S. Arott, J. F. Cochran, S. T. Purcell, K. B. Urquhart, and K. Myrtle, J. Cryst. Growth **81**, 562 (1987); B. Heinrich, A. S. Arrott, J. F. Cochran, C. Liu, and K. Myrtle, J. Vac. Sci. Technol. A **4**, 1376 (1986).

[6]B. Heinrich, S. T. Purcell, J. R. Dutcher, K. B. Urquhart, J. F. Cochran, and A. S. Arrott, Phys. Rev. B **38**, 12 879 (1986).

[7]V. L. Moruzzi, P. M. Marcus, K. Schwarz, and P. Mohn, Phys. Rev. B **34**, 1784 (1986); V. L. Moruzzi, Phys. Rev. Lett. **57**, 2211 (1986); V. L. Moruzzi and P. M. Marcus, Phys. Rev. B **38**, 1613 (1988).

[8]C. L. Fu, A. J. Freeman, and T. Oguchi, Phys. Rev. Lett. **54**, 2700 (1985).

[9]J. I. Lee, S. C. Hong, and A. J. Freeman (unpublished).

[10]J. A. C. Bland, R. D. Bateson, A. D. Johnson, B. Heinrich, Z. Celinski, and H. J. Lauter, J. Magn. Magn. Mater. **93**, 331 (1991).

[11]P. D. Johnson, S. L. Hulbert, R. Klaffky, N. B. Brookes, A. Clarke, B. Sinković, N. V. Smith, R. Celotta, M. H. Kelly, D. T. Pierce, M. R. Scheinfein, B. J. Waclawski, and M. R. Howells, Rev. Sci. Instrum. **63**, 1902 (1992).

[12]J. Unguris, D. T. Pierce, and R. J. Celotta, Rev. Sci. Instrum. **57**, 1314 (1986).

[13]E. Kisker, K. Schroder, W. Gudat, and M. Campagna, Phys. Rev. B **31**, 329 (1985).

[14]D. A. Papaconstantopoulos, *Handbook of the Band Structure of Elemental Solids* (Plenum, New York, 1986).

[15]O. K. Andersen and O. Jepsen, Physica **91B**, 317 (1977); O. K. Andersen, W. Klose, and H. Nohl, Phys. Rev. B **17**, 1209 (1978).

[16]W. Eberhardt and E. W. Plummer, Phys. Rev. B **21**, 3245 (1980).

[17]G. Tréglia, F. Ducastelle, and D. Spanjaard, J. Phys. (Paris) **43**, 341 (1981).

[18]E.g., S. Hufner and G. K. Wertheim, Phys. Rev. Lett. **51A**, 299 (1975).

[19]C. Guillot, Y. Ballu, J. Paigne, J. Lecante, R. P. Jain, P. Thiry, R. Pinchaux, Y. Petroff, and L. M. Falicov, Phys. Rev. Lett. **39**, 1632 (1977).

[20]R. Clauberg, W. Gudat, E. Kisker, E. Kuhlmann, and G. M. Rothberg, Phys. Rev. Lett. **47**, 1314 (1981).

[21]D. P. Pappas, K.-P. Kämper, B. P. Miller, H. Hopster, D. E. Fowler, C. R. Brundle, A. C. Luntz, and Z.-X. Shen, Phys. Rev. Lett. **66**, 504 (1991).

[22]S. Tanuma, C. J. Powell, and D. R. Penn, J. Electron. Spectrosc. Relat. Phenom. **52**, 285 (1990).

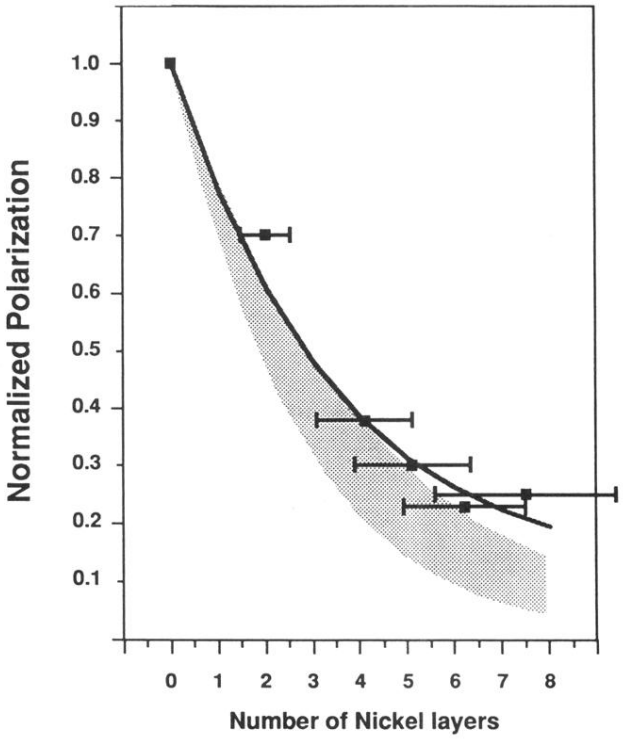

FIG. 4. Normalized polarization, $P(x)/P_s$ [see Eq. (1)], as a function of overlayer thickness for bcc nickel grown on Fe(001). The squares represent the experimental points. The horizontal error bars are shown, and the vertical error bars are less than the symbols. The shaded region gives the expected results assuming a nonmagnetic overlayer with a range of mean free paths (λ), $\lambda = 4.5 \pm 1$ Å, and the solid line gives the result assuming a small nickel moment; see the text for details.